Elementary Steps of Initiation and Termination Processes in Radical Polymerization

Michael Buback

Institut für Physikalische Chemie der Georg-August-Universität Göttingen
Tammannstraße 6, 37077 Göttingen, Germany
E-mail: mbuback@gwdg.de

Summary: Investigations into the kinetics of primary radicals produced in photochemically and thermally induced decomposition of peroxides of type $R_1C(O)O\text{-}OR_2$ are presented. The correlation of peroxide structure with decomposition rate and with initiator efficiency in radical polymerizations is discussed. Termination rate coefficients, k_t, as a function of temperature, pressure, polymer content, and of chain length may be deduced from two types of time-resolved experiments in which, after applying an excimer laser pulse, either monomer conversion is measured via near-infrared spectroscopy or the decay in radical concentration is monitored via electron spin resonance.

Keywords: initiator efficiency; kinetics (radical polym.); peroxides; pulsed laser polymerization; termination

Introduction

Modeling monomer conversion vs. time profiles and product properties for free-radical polymerizations requires detailed knowledge about the rate coefficients of the relevant individual reaction steps. Propagation rate coefficients, k_p, may be accurately obtained via the pulsed laser polymerization – size-exclusion chromatography (PLP–SEC) method. The addition of a monomer molecule to a propagating radical occurs under chemical control in most cases. Thus, k_p is less dependent or is even independent of physical properties of the polymerizing medium, such as polymer content, polymer microstructure, and free-radical size. Termination of two macroradicals, on the other hand, and to a certain extent also combination and disproportionation reactions of small radicals subsequent to their formation by initiator decomposition, are diffusion controlled and thus may significantly depend on the physical properties of the reaction medium.

Part I of this paper addresses initiation processes of peroxide species of type $R_1C(O)OOR_2$ (see Figure 1) including peroxyesters, diacyl peroxides, and peroxycarbonates with part of the kinetic data being derived with ps or even sub-ps time resolution. Part II addresses termination rate coefficients, k_t, in free-radical polymerization and, in particular, the chain-length dependence of k_t. Termination rate coefficients are deduced from two types of laser-

 DOI: 10.1002/masy.200550812

assisted techniques. The focus will be on a novel experiment in which the decay of radical concentration after instantaneous laser-pulse-induced generation of a significant amount of primary photoinitiator-derived radicals is measured via ESR spectroscopy.

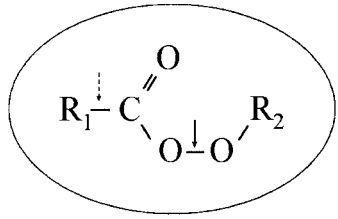

Figure 1. Structure of the peroxides under investigation.

Results and discussion

I. Elementary steps of initiation

Shown in Figure 1 is the general formula of the peroxides under investigation. Analysis of the temperature and pressure dependence of initiator decomposition rate in dilute solution of *n*-heptane[1] provides evidence on the decomposition mode, which may be by single-bond scission of the peroxy linkage or by concerted (or extremely rapid successive) scission of two bonds, accompanied by CO_2 formation. The decomposition mechanism, via single-bond or two-bond scission, bears important consequences for initiator efficiency in radical polymerization.[2] In case of close-to-concerted two-bond scission and thus of simultaneous CO_2 formation, subsequent cage combination or disproportionation reactions of the produced radicals lead to relatively stable products, e.g., to an ether in case of radical combination of the primary radicals produced from peroxyester decomposition. Such components will not decompose under typical polymerization conditions and the loss in primary radical concentration upon their formation may be associated with a significant reduction in overall initiator efficiency. In case of single-bond scission, on the other hand, in-cage recombination restores the peroxyester molecule, which may undergo another decomposition step and therefore may finally result in addition of primary radicals to monomer molecules and thus in formation of growing radicals.

Because of the close correlation of initiator decomposition kinetics and mechanism, it is of primary importance to obtain detailed insight into the in-cage processes subsequent to primary bond dissociation. UV pump–VIS/nearIR/midIR probe experiments with time resolution in the fs and ps range are perfectly suited for this purpose.[3-5] Shown in Figure 2

are concentration vs. time profiles of intermediate and product species occurring after photo-dissociation of *tert*-butyl 2-naphthyl peroxycarbonate measured via highly time-resolved pump-probe techniques.[3,4] The time dependence of the decay of intermediate naphthyloxy carbonyloxy (NOCO) radicals and the production of naphthyloxy radicals and of CO_2 yields identical rates for NOCO decomposition. Whereas thermal NOCO decomposition is a ps process at ambient temperature, the decomposition of radicals with the carbonyloxy moiety being directly linked to an aromatic ring, e.g., of naphthyl carbonyloxy radicals, occurs over a significant barrier (see Figure 3) on a nano- or even microsecond time scale, after energy relaxation to ambient conditions.[6] Concentration vs. time traces as in Figure 2 may be adequately analyzed by a semi-quantitative model[5] based on unimolecular rate theory and on density functional theory (DFT).

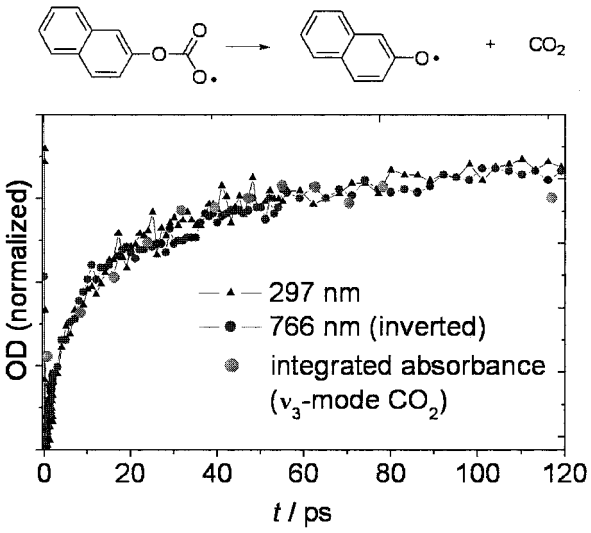

Figure 2. Highly time-resolved absorbance (optical density, OD) measurement of naphthyloxy carbonyloxy decay (at 766 nm) and of naphthyloxy and CO_2 production, monitored at 297 nm and in the IR, respectively, after photo-dissociation of *tert*-butyl 2-naphthyl peroxycarbonate.[3,4]

Barriers to decomposition for radicals with and without an oxygen atom (or a CH_2 group) between the carbonyloxy moiety and the aromatic system have been estimated by DFT calculations, see Refs.[5,7] For naphthyl carbonyloxy and for phenyloxy carbonyloxy radicals, the calculated barriers are shown in Figure 3.

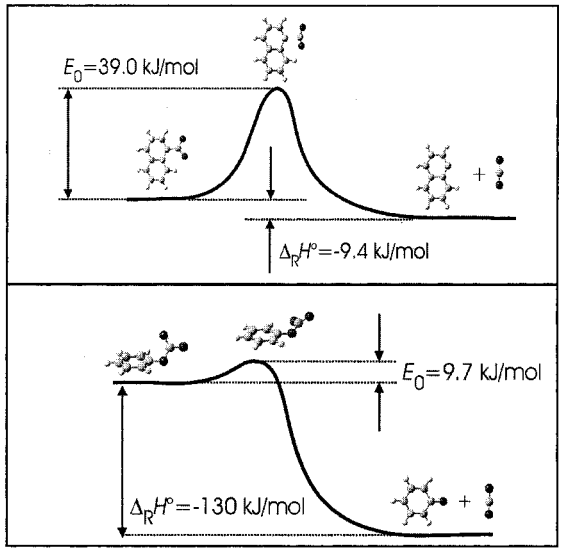

Figure 3. Barriers to decomposition for naphthyl carbonyloxy (upper part) and for phenyloxy carbonyloxy (lower part) radicals.[7]

The time scale of decarboxylation of primary carbonyloxy radicals significantly affects cage combination processes and thus initiator efficiency. In case of close-to-concerted two-bond scission of a peroxyester associated with CO_2 formation, as with peroxypivalates, a carbon-centered and an oxygen-centered radical are produced, which may very rapidly react with each other, e.g., by an in-cage disproportionation to *iso*-butene and *tert*-butanol after *tert*-butyl peroxypivalate (TBPP) photo-dissociation. As a consequence, the initiator efficiency of TBPP is rather low, e.g., around 0.4 in ethene homopolymerization at pressures of 2000 bar.[2,8] The very rapid decarboxylation of the pivaloyl carbonyloxy radical is a β-scission process that is driven by the low energy of the produced *tert*-butyl radical. On the other hand, the methyl carbonyloxy radical produced during peroxyacetate decomposition does slowly dissociate, as the methyl radical is relatively high in energy. Also with peroxyacetates, however, the situation of an oxygen-centered radical occurring together with a (carbon-centered) *tert*-butyl radical may be produced by appropriate selection of the so-called "alcohol side" of the peroxyester. As is illustrated in Scheme 1, the primary dissociation step of tetramethylpropyl peroxyacetate (TMPPA) produces an oxygen-centered radical which may rapidly decompose via a β-scission reaction to acetone and to a *tert*-butyl radical with, again, the stability of the tertiary radical (and of acetone) being the driving force behind this process. Because of in-

cage production of a *tert*-butyl radical and an oxygen-centered radical from both TBPP and TMPPA it comes as no surprise that the initiator efficiency of both peroxides has been found to be close to 0.4 in ethene high-pressure polymerization.[2,9]

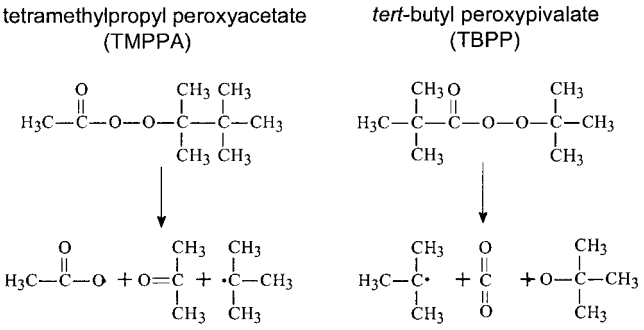

Scheme 1. Intermediate in-cage products from TMPPA and TBPP decomposition.

Although cage escape of radicals in most cases results in successful initiation, it is by no means clear, whether the radical which leaves the primary caged situation will be the species that actually initiates polymerization. There may be follow-up decomposition reactions or chain-transfer processes, to monomer, to solvent or to specific chain-transfer molecules, which change the type of free radical during the time interval prior to the addition to a monomer molecule. This interval may extend at least up to a few microseconds, but may also expand up to several milliseconds. It is important to know, in particular for polymerization to lower molecular weight material, which radicals start the growing chain, thereby becoming end groups of the polymer.

To identify such end groups, electrospray-ionization mass spectrometry (ESI-MS) has been used.[10] The method provides detailed insight into the reactions of free radicals in the time range of nanoseconds to milliseconds. Shown in Figure 4 is the simple situation seen in the ESI-MS spectrum for the mass range of one repeat unit of methyl methacrylate polymer produced with tetramethylpropyl peroxypivalate (TMPPP) as the initiator. TMPPP consists of the "acid side" of TBPP and the "alcohol side" of TMPPA (Scheme 1).

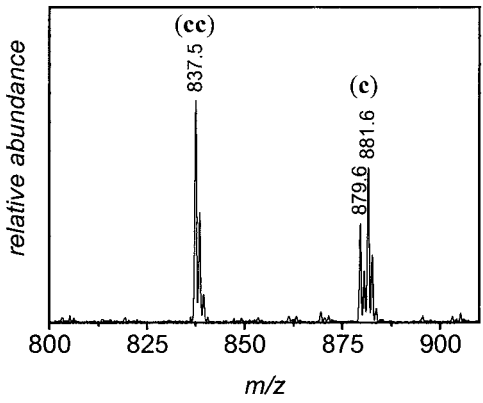

Figure 4. ESI-MS spectrum of poly(MMA) initiated by 1,1,2,2-tetramethylpropyl peroxypivalate (TMPPP) in toluene at 90 °C. The *m/z*-range covers one monomer repeat unit.[10] The notation **c** characterizes one *tert*-butyl end group (see text).

Only *tert*-butyl moieties, referred to as **c**, are observed as end groups. The notation (**cc**) indicates that the polymer molecule contains two such *tert*-butyl moieties as a consequence of termination by combination of two growing radicals, each of which bears one **c** unit, whereas (**c**) indicates that the polymer molecule contains only one *tert*-butyl moiety. The latter product results from termination by disproportionation. Closer inspection indicates, that signal (**c**) actually consists of two components with masses differing by two units, as is to be expected for termination events by disproportionation. The additional fine structure with a spacing of one mass unit is due to part of the polymeric species containing ^{13}C-atoms. In order to allow for ESI–MS analysis, the molecular weight has been kept low by using significant amounts of initiator. The mass range depicted in Figure 4 refers to "poly(methyl methacrylate)" made up of eight monomer units. The type of signal is repetitively seen for "polymer" with less and with more (up to 20) MMA units (see [10]). More complex ESI–MS spectra, as are occurring in polymerizations where two or three types of free radicals start macromolecular growth, are presented in Ref. [10] Within these spectra, polymer with one out of the several types of end groups and with all binary combinations of end groups are seen and may be safely assigned. Future work will also address the disproportionation-to-combination ratio of termination processes that may be deduced from the ESI–MS spectra.

II. Chain-length dependence of free-radical termination

Laser single-pulse (SP) experiments are well suited for measuring termination rate coefficients, k_t, including the determination of the dependence of k_t on monomer

conversion and on chain length. An excimer laser single pulse may be applied for instantaneously producing a significant concentration of photoinitiator-derived primary radicals, c_R^0. Subsequent time-resolved NIR spectroscopic measurement of monomer concentration, via the so-called SP–PLP (or, more precisely, SP–PLP–NIR method) yields the termination rate coefficient for a narrow interval of monomer conversion, typically well below 0.1 %.[11] Successive SP–PLP–NIR experiments may be carried out during the course of a polymerization, thus providing a point-wise probing of termination kinetics up to moderate or even high degrees of monomer conversion. Alternatively, within the novel SP–PLP–ESR experiment that will be discussed further below, the decay of free-radical concentration after applying the laser pulse is measured and a direct access to the termination kinetics is thus provided.

In case that ideal kinetics applies with a single (chain-length independent) value of k_t, the primary quantity from SP–PLP–NIR, which is the ratio of termination to propagation rate coefficients, k_t/k_p, is easily converted into k_t by introducing the value for k_p from independent PLP-SEC experiments. Termination rate is, however, chain-length dependent and the k_t values derived from SP–PLP–NIR by the procedure just outlined, should properly be referred to as the time and chain-length averaged termination rate coefficients, $\langle k_t \rangle$. Actually, as radical chain length increases linearly with time t after applying the pulse, termination occurs between two radicals of almost identical size i, unless chain-transfer reactions come into play. The adequate expression for termination in SP–PLP experiments therefore reads:

$$-\frac{dc_R}{dt} = 2 \cdot k_t(i,i) \cdot c_R^2 \qquad (1)$$

Because of the above-mentioned linear correlation of time t after the pulse with the narrowly distributed chain length i of propagating radicals at this particular time t, the detailed analysis of the monomer concentration vs. time profile allows for estimating $k_t(i,i)$. In order to provide a model-free determination of $k_t(i,i)$ from c_M vs. t traces, a two-fold differentiation of the experimental material is required. The quality of the data is not sufficiently high to allow for a reasonable such two-fold differentiation. For this reason, the frequently used model expression in Eq. (2) has been introduced for describing chain-length dependent $k_t(i,i)$ via the parameters k_t^0 and α:

$$k_t(i,i) = k_t^0 \cdot i^{-\alpha} \qquad (2)$$

where k_t^0 characterizes the rate coefficient for termination of two very small radicals and α represents the extent of chain-length dependence.

Shown in Figure 5 are α values deduced from SP–PLP–NIR experiments carried out on several acrylate and methacrylate homopolymerizations.[12]

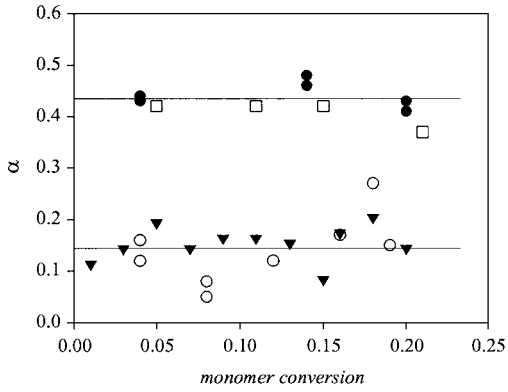

Figure 5. Power-law exponents α representing the chain-length dependence of the termination rate coefficient in bulk polymerizations of dodecyl acrylate (squares), ethylhexyl acrylate (full circles), butyl acrylate (triangles), and dodecyl methacrylate (open circles) at 1000 bar, 40°C and monomer conversions up to 20 per cent.[12]

The α values reported in Figure 5 have been determined from the chain-length region up to several thousand monomer units, but essentially refer to $100 < i < 1000$, as the change in monomer concentration is very steep at lower i and is very small at higher i with both these effects posing problems for an accurate analysis. In order to improve the signal-to-noise ratio of the microsecond time-resolved nearIR-spectroscopic detection of monomer conversion, the experiments have been carried out at 40°C and high pressure (1000 bar). In the monomer conversion region up to 20 per cent, α stays more or less constant. Interestingly, however, two levels of α are observed, a higher one at around 0.43 and a lower one, at around 0.16. The higher value, which is observed for acrylic acid esters with long alkyl chains, is assigned to significant contributions of mid-chain radicals to termination, whereas the lower (classical) value of α, close to 0.16, corresponds to termination of radicals with the radical functionality being located at or close to the chain terminus. These assignments are consistent with predictions from theory.[13]

In order to directly access termination rate, the decay of radical concentration, c_R, after applying a laser pulse should be measured rather than the decrease in monomer

concentration which latter quantity is monitored in the SP–PLP–NIR experiment. c_R vs. t traces are provided by the novel SP–PLP–ESR experiment. Shown in Figure 6 is the time dependence of reduced radical concentration, c_R/c_R^0, measured during a dodecyl methacrylate (DMA) bulk polymerization at 0°C, ambient pressure, and at 14 per cent monomer conversion (which results from polymerization induced by preceding laser pulses).[14] To reach the signal-to-noise quality of the trace in Figure 6, 20 individual single pulse experiments have been co-added. The monomer conversion interval covered during the period of taking these 20 traces is below 2 per cent.

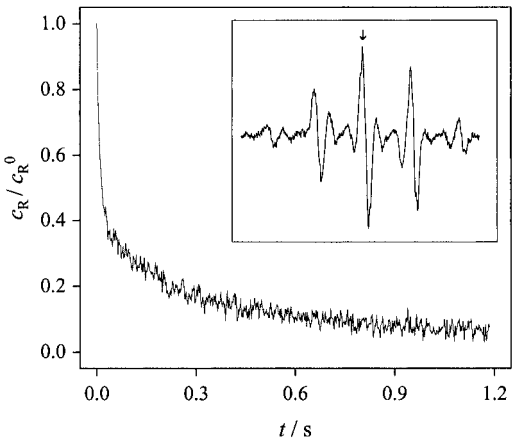

Figure 6. Time dependence of reduced radical concentration, as measured via ESR, after applying a laser pulse in dodecyl methacrylate bulk polymerization at 0°C, ambient pressure, and at 14 per cent monomer conversion from preceding polymerization. c_R^0 refers to the initial pulse-induced free-radical concentration.[14] The insert shows the full ESR spectrum of the DMA macroradical. The field position where time-resolved analysis has been carried out is indicated by the arrow.

Integration of Eq. (1) under the assumption of termination being independent of chain length, $k_t(i,i) = k_t$, yields Eq. (3):

$$\frac{c_R(t)}{c_R^0} = \left(1 + 2 \cdot k_t c_R^0 t\right)^{-1} \tag{3}$$

which however, as is to be expected, allows for no good fit of the experimental data in Figure 6. For this reason, Eq. (2) is inserted into Eq. (1) and, after integration, Eq. (4) is obtained:

$$\frac{c_R(t)}{c_R^0} = \left(\frac{2 \cdot k_t^0 \cdot c_R^0 \cdot t_p^\alpha}{1-\alpha} \cdot t^{(1-\alpha)} + 1 \right)^{-1} \quad (4)$$

where $t_p = (k_p \cdot c_M)^{-1}$ is the so-called propagation time, that is the average time interval between two successive propagation steps. Fitting of the data in Figure 6 results in a rather satisfactory representation with the exception of the very early time region, $0 < t < 0.3$ s. The exponent obtained from this fitting procedure for the chain-length interval $1 < i < 1000$ is: $\alpha = 0.34$. To get a clearer perspective of the quality of fits by the model underlying Eq. (4), double-log plots of the inverse of $c_R(t)/c_R{}^0$, that is of $c_R{}^0/c_R(t)$, have been made. Eq. (5) tells, that plotting $\log(c_R{}^0/c_R(t) - 1)$ vs. $\log t$ should result in a straight line of slope $(1-\alpha)$ in case that termination kinetics follows the power-law expression (Eq. 2) with a single exponent α.

$$\frac{c_R^0}{c_R(t)} - 1 = C \cdot t^{(1-\alpha)} \quad (5)$$

where the constant is $C = (2 \cdot k_t^0 \cdot c_R^0 \cdot t_p^\alpha)/(1-\alpha)$. The resulting double-log plot for the data from Figure 6 is given in Figure 7. Obviously, no single straight line is capable of fitting the radical concentration vs. time profile. As has been outlined in Ref.[14], the two straight lines (in Figure 7) that provide an excellent representation of the experimental data within the entire experimental time (and thus chain-length) region, indicate that two exponents α apply. The chain-length dependence is larger, around $\alpha = 0.5$, at chain lengths up to about $i = 100$, and is significantly smaller above $i = 100$, where α is close to the value determined via SP–PLP–NIR (see Figure 5) and is close to the theoretical value for termination of large-size radicals with chain-end functionality.[13]

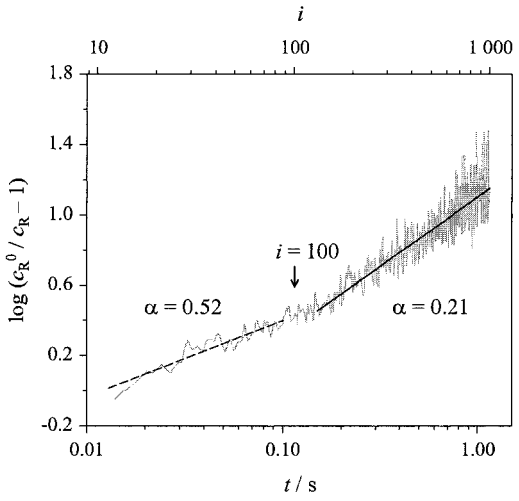

Figure 7. Double-log plot, according to Eq. (5), of the DMA trace depicted in Figure 6. The straight lines are adjusted to the chain-length intervals $8 < i < 100$ (---) and $100 < i < 1000$ (—), respectively.

That the chain-length dependence of k_t is larger at small chain lengths and vice versa, has already been suggested within the framework of the "composite model" in Ref.[15] (where also earlier evidence on this aspect is summarized). It should particularly be noted that the absolute values of α predicted for the low and high chain-length regimes in Ref.[15] are almost identical to the ones that result from analysis, via Eqs. (4) and (5), of the radical concentration vs. time traces measured for DMA via SP–PLP–ESR. In addition, the cross-over region from the behavior at low i to the one at high i occurs at about the same value of i that has been suggested in presenting the composite model.[15]

The analysis for chain-length dependence of k_t from SP–PLP–ESR presented so far, still uses the model expression for $k_t(i,i)$ from Eq. (2). Within recent SP–PLP–ESR studies into *n*-butyl itaconate polymerization, it has been shown that also a model-free approach may be used to determine $k_t(i,i)$.[16] To do so, an arbitrary mathematical function has been used to perfectly fit the experimental $c_R(t)/c_R^0$ vs. t traces. The resulting expression is then differentiated according to Eq. (1) to yield $k_t(i,i)$. The results from the model-dependent and from the model-independent approach are in close agreement. The SP–PLP–ESR technique is particularly well suited for investigations into lower-k_p and lower-k_t monomers. The high signal quality even allows for distinguishing termination behavior of small radicals from the one of large-size radicals. For high-k_p and high-k_t monomers, the SP–PLP–NIR shows more promise, at least with the currently available instrumentation. It

appears to be a matter of priority to further improve the techniques in order to allow for application of both methods to as many as possible types of monomers.

Conclusions

Pulsed laser experiments in conjunction with highly time-resolved measurements, via IR or VIS and via NIR or ESR detection, respectively, provide detailed insight into initiation and termination processes in free-radical polymerization. The initiator decomposition studies are accompanied by DFT calculations and by ESI-MS measurements. A novel SP–PLP–ESR experiment is presented which allows for measuring termination rate coefficients as a function of monomer conversion and of chain length.

Acknowledgements

The individual research projects underlying this overview have been generously supported by the *Deutsche Forschungsgemeinschaft*. The author is grateful to AKZO NOBEL for the cooperation in the area of peroxide decomposition and initiator efficiency. Support by *Dr. Philipp Vana* in finalizing the manuscript is gratefully acknowledged.

[1] M. Buback, J. Sandmann, *Z. Phys. Chem.* **2000**, *214*, 583.
[2] P. Becker, M. Buback, J. Sandmann, *Macromol. Chem. Phys.* **2002**, *203*, 2113.
[3] J. Aschenbrücker, M. Buback, N. P. Ernsting, J. Schroeder, U. Steegmüller, *Ber. Bunsenges. Phys. Chem.* **1998**, *102*, 965.
[4] B. Abel, J. Assmann, M. Buback, Ch. Grimm, M. Kling, S. Schmatz, J. Schroeder, T. Witte, *J. Phys. Chem. A* **2003**, *107*, 9499.
[5] M. Buback, M. Kling, S. Schmatz, J. Schroeder, *Phys. Chem. Chem. Phys.* **2004**, *6*, 5441.
[6] B. Abel, J. Aßmann, M. Buback, M. Kling, S. Schmatz, J. Schroeder, *Angew. Chem. Int. Ed.* **2003**, *42*, 299.
[7] M. Kling, S. Schmatz, *Phys. Chem. Chem. Phys.* **2003**, *5*, 3891.
[8] M. Buback, *Macromol. Symp.* **2002**, *182*, 103.
[9] S. Hinrichs, *Diplomarbeit*, Göttingen 2000.
[10] M. Buback, H. Frauendorf, P. Vana, *J. Polym. Sci. Part A:Polym. Chem.* **2004**, *42*, 4266.
[11] M. Buback, H. Hippler, J. Schweer, H. P. Vögele, *Makromol. Chem., Rapid Commun.* **1986**, *7*, 261; S. Beuermann, M. Buback, *Prog. Polym. Sci.* **2002**, *27*, 254.
[12] M. Buback, M. Egorov, A. Feldermann, *Macromolecules* **2004**, *37*, 1768.
[13] B. Friedman, B. O'Shaughnessy, *Macromolecules* **1993**, *26*, 5726.
[14] M. Buback, M. Egorov, T. Junkers, E. Panchenko, *Macromol. Rapid Commun.* **2004**, *25*, 1004.
[15] G. B. Smith, G. T. Russell, J. P. A. Heuts, *Macromol. Theory Simul.* **2003**, *12*, 299.
[16] M. Buback, M. Egorov, T. Junkers, E. Panchenko, *Macromol. Chem. Phys.* **2005**, *206*, 333.